

## First Season of Operation of the TAIGA Hybrid Cherenkov Array

L. G. Sveshnikova<sup>a,\*</sup>, I. I. Astapov<sup>b</sup>, P. A. Bezyazeev<sup>c</sup>, V. Boreyko<sup>d</sup>, A. N. Borodin<sup>d</sup>, M. Brueckner<sup>e</sup>,  
N. M. Budnev<sup>c</sup>, A. Chiavassa<sup>f</sup>, A. N. Dyachok<sup>c</sup>, O. L. Fedorov<sup>c</sup>, A. R. Gafarov<sup>c</sup>, A. Yu. Garmash<sup>g,h</sup>,  
N. V. Gorbunov<sup>d</sup>, V. M. Grebenyuk<sup>d,i</sup>, O. A. Gress<sup>c</sup>, T. I. Gress<sup>c</sup>, O. G. Grishin<sup>c</sup>, A. A. Grinyuk<sup>d</sup>,  
D. Horns<sup>j</sup>, A. L. Ivanova<sup>c</sup>, N. N. Kalmykov<sup>a</sup>, Y. A. Kazarina<sup>c</sup>, V. V. Kindin<sup>b</sup>, S. N. Kiryuhin<sup>c</sup>,  
P. S. Kirilenko<sup>g</sup>, R. P. Kokoulin<sup>b</sup>, K. G. Kompaniets<sup>b</sup>, E. E. Korosteleva<sup>a</sup>, V. A. Kozhin<sup>a</sup>,  
E. A. Kravchenko<sup>g,h</sup>, M. Kunas<sup>j</sup>, A. A. Lagutin<sup>k</sup>, L. A. Kuzmichev<sup>a</sup>, Yu. Lemeshev<sup>c</sup>, V. V. Lenok<sup>c</sup>,  
B. K. Lubsandorzhev<sup>l</sup>, N. B. Lubsandorzhev<sup>a</sup>, R. R. Mirgazov<sup>c</sup>, R. Mirzoyan<sup>m,c</sup>, R. D. Monkhoev<sup>c</sup>,  
E. A. Osipova<sup>a</sup>, A. L. Pakhorukov<sup>c</sup>, M. I. Panasyuk<sup>a</sup>, L. V. Pankov<sup>c</sup>, A. A. Petrukhin<sup>b</sup>, V. A. Poleschuk<sup>c</sup>,  
M. Popescu<sup>n</sup>, E. G. Popova<sup>a</sup>, A. Porelli<sup>e</sup>, E. B. Postnikov<sup>a</sup>, V. V. Prosin<sup>a</sup>, V. S. Ptuskin<sup>o</sup>, E. V. Rjabov<sup>c</sup>,  
G. I. Rubtsov<sup>l</sup>, A. A. Pushnin<sup>c</sup>, R. I. Raikin<sup>k</sup>, Y. I. Sagan<sup>d,i</sup>, B. M. Sabirov<sup>d</sup>, V. S. Samoliga<sup>c</sup>,  
Yu. A. Semenyev<sup>c</sup>, A. A. Silaev<sup>a</sup>, A. A. Silaev, Jr.<sup>a</sup>, A. Yu. Sidorenkov<sup>l</sup>, A. V. Skurikhin<sup>a</sup>,  
M. Slunicka<sup>d</sup>, A. V. Sokolov<sup>g,h</sup>, C. Spiering<sup>e</sup>, V. A. Tabolenko<sup>c</sup>, B. A. Tarashansky<sup>c</sup>,  
A. V. Tkachenko<sup>d</sup>, L. G. Tkachev<sup>d,i</sup>, M. Tluczykont<sup>j</sup>, R. Wischnewski<sup>e</sup>,  
A. V. Zagorodnikov<sup>c</sup>, D. P. Zhurov<sup>c</sup>, V. L. Zurbanov<sup>c</sup>, and I. I. Yashin<sup>b</sup>

<sup>a</sup>Skobeltsyn Institute of Nuclear Physics, Moscow State University, Moscow, 119991 Russia

<sup>b</sup>National Research Nuclear University MEPhI (Moscow Engineering Physics Institute), Moscow, 115409 Russia

<sup>c</sup>Research Institute of Applied Physics, Irkutsk State University, Irkutsk, 664003 Russia

<sup>d</sup>Joint Institute for Nuclear Research, Dubna, Moscow oblast, 141980 Russia

<sup>e</sup>Deutsches Elektronen-Synchrotron DESY, Zeuthen, 15738 Germany

<sup>f</sup>Department of Physics, University of Torino and Istituto Nazionale di Fisica Nucleare, Torino, 10125 Italy

<sup>g</sup>Novosibirsk State University, Novosibirsk, 630090 Russia

<sup>h</sup>Budker Institute of Nuclear Physics, Siberian Branch, Russian Academy of Sciences, Novosibirsk, 630090 Russia

<sup>i</sup>Dubna University, Dubna, Moscow oblast, 141980 Russia

<sup>j</sup>Institut für Experimentalphysik, Universität Hamburg, Hamburg, D-22 761 Germany

<sup>k</sup>Altai State University, Barnaul, Altai krai, 656049 Russia

<sup>l</sup>Institute for Nuclear Research, Russian Academy of Sciences, Moscow, 117312 Russia

<sup>m</sup>Max Planck Institute for Physics, Munich, 80805 Germany

<sup>n</sup>Space Science Institute, Magurele, 077125 Romania

<sup>o</sup>Pushkov Institute of Terrestrial Magnetism, the Ionosphere, and Radio Wave Propagation, Russian Academy of Sciences, Troitsk, Moscow, 142190 Russia

\*e-mail: tf110@mail.ru

Received October 10, 2018; revised February 20, 2019; accepted April 26, 2019

**Abstract**—Work is currently under way in the Tunka Valley, 50 km from Lake Baikal, to create the TAIGA gamma observatory for studying gamma radiation and cosmic ray fluxes in the  $10^{13}$ – $10^{18}$  eV range of energies. To detect gamma rays with energies above tens of TeV, a hybrid method of detecting showers is implemented. It is based on data obtained by the TAIGA Imaging Atmospheric Cherenkov Telescope (IACT) and the wide-angle TAIGA-HiSCORE array. The preliminary results from processing the telescope's data for the low-energy region ( $>2$ – $3$  TeV) are presented. Joint events with energy more than 50 TeV are analyzed and compared to Monte Carlo calculations.

DOI: 10.3103/S1062873819080379

### INTRODUCTION

The TAIGA gamma observatory [1–6] (Tunka Advanced Instrument for cosmic ray physics and Gamma-ray Astronomy) is now operating in the Tunka Valley, 50 km from Lake Baikal. The observatory is designed to study gamma radiation and charged

cosmic ray fluxes in the energy range of  $10^{13}$ – $10^{18}$  eV. The structure of the observatory includes the TAIGA-HiSCORE array (which as of August 2018 consisted of 43 stations covering an area of  $0.4 \text{ km}^2$ ) [7]. A hybrid method of detecting gamma quanta was proposed and validated in the TAIGA experiment [3], in which

TAIGA-HiSCORE was supplemented with several imaging atmospheric Cherenkov telescopes (IACTs) located fairly wide distances (up to 600 m) from one another [3]. The first IACT, positioned approximately in the center of the TAIGA-HiSCORE array, was commissioned in 2017 and is now fully operational.

### TAIGA-IACT ARRAY

The TAIGA-IACT telescope is equipped with a composite Davies–Cotton mirror consisting of 29 segments with a total area of 8.5 m<sup>2</sup> and a focal length of 4.75 m. A sensitive camera with 560 PMTs, each of which has a photocathode diameter of around 19 mm, is installed at the focus of the mirrors. The diameter of the camera is approximately 110 cm. The camera's viewing angle is 9.6°, and the viewing angle of each pixel is 0.36°. The camera was assembled from similar clusters, generally with 28 PMTs each (the number of PMTs in the clusters at the edge of the camera is fewer than 28). The readout system and the trigger system were described in [1, 11].

The calibration of the camera, i.e. the determination of the relative sensitivity of PMTs and the coefficients for recalculating from the ADC codes to the number of photoelectrons (PE), was done according to the calibration files obtained when the camera responded to a pulsed light source [8].

### RECONSTRUCTING THE EVENTS AND STATISTICS OF THE 2017–2018 SEASON

The observations with the telescope were made from October to March (118 days), with the time divided between the two main test sources: the nearest blazar Mkr421 (90 h from January to March) and the Crab Nebula (176 h from October to February). For a number of reasons, however, only around 25 h of observations were used in processing. The total trigger count rate depended on the weather and snow cover and averaged at approximately 1 KHz; the count rate of the events in which the EAS signal was recorded was approximately 16 Hz; and the count rate of joint events (with EAS signals recorded simultaneously by the telescope and TAIGA-HiSCORE array) was approximately 0.3 Hz. The procedure for reconstructing events consisted of several steps:

(a) From the events accumulated every 2 min of the camera's operation, the average pedestal values and standard deviation  $\sigma_i$  are reconstructed for all channels of the camera. These pedestal values are used to form amplitude matrix  $Am(X_i, Y_i)$  (where  $X_i$  and  $Y_i$  are the pixel coordinates) for the events recorded over those 2 min.

(b) Using the values of anode currents measured every 30 s, the background light is monitored and the quality of events is analyzed; unstable pixels and pixels with light from the stars are excluded. Corrections are

introduced for the source position deviating from the center of the camera in a given night.

(c) The image is cleaned of noise (cleaning procedure) from the pixels in which the signal amplitude comes from fluctuations in the light background. A pixel is included in the EAS image and selected if the amplitude exceeds specified value  $N_1$  PE, and is greater than  $N_2$  PE in at least one neighboring pixel ( $N_2 = 1/2 N_1$ ). The choice of  $N_1$  depends on the run (measuring cycle) and is chosen as  $(3-5) \times \sigma_i$ , where  $\sigma_i$  is the standard deviation of the pedestal for a given pixel. In this approach, values  $N_1$  and  $N_2$  differ for different pixels. Total number  $N_{\text{pix}}$  of pixels included in the image, and total number  $S$  (size) of photoelectrons in the image are also determined.

(d) The Hillas parameters [10] are determined from matrix  $Am(X_i, Y_i)$ :  $R_c$  is the distance from the center of the image to the center of the camera (*dist*);  $W$  is width,  $L$  is length,  $Con$  is concentration, and  $\alpha$  is the angle between the major axis of the Hillas ellipse and the vector oriented from the center of gravity of the image to the center of the camera. Images are selectively visualized to verify the quality of events.

(e) A search is performed for time-coincident (time window, 1.5  $\mu$ s) events from the banks of those detected by the IACT and TAIGA-HiSCORE array. The selected joint events are assigned energy  $E$ , azimuth and zenith angles  $\theta$  and  $\varphi$ , distance  $R_p$  to the shower axis from the telescope, and angle  $\Theta$  between the direction of the shower and the direction to the source. These parameters are obtained from the TAIGA-HiSCORE array data using the approach described in [2, 4, 5].

Study of the amplitude spectra of individual pixels shows that the value of  $N_1$  in cleaned events can be chosen as  $3\sigma_i$  (~6–8 PE).

During observations of the Crab Nebula (CN), 1.8 million events were recorded in an effective time of 25 h. For the observations of source Mkr421 in March 2018, the effective time was 20 h.

The search for joint events was conducted only during observations of the CN. So far, only events recorded by the first cluster of the TAIGA-HiSCORE array have been analyzed.

### MONTE CARLO SIMULATIONS AND COMPARISON TO THE EXPERIMENT

Simulations using the Monte Carlo (MC) approach were performed using the CORSIKA 7.3500 software (IACT option). The configuration of the detectors corresponded to the array of 2017 (i.e., one telescope and 30 stations of the first cluster). Cherenkov photons were passed through the telescope's optical system (mirrors and a PMT matrix with Winston cones) using the Optics program developed for the TAIGA experiment by A.N. Grinyuk (Joint Institute

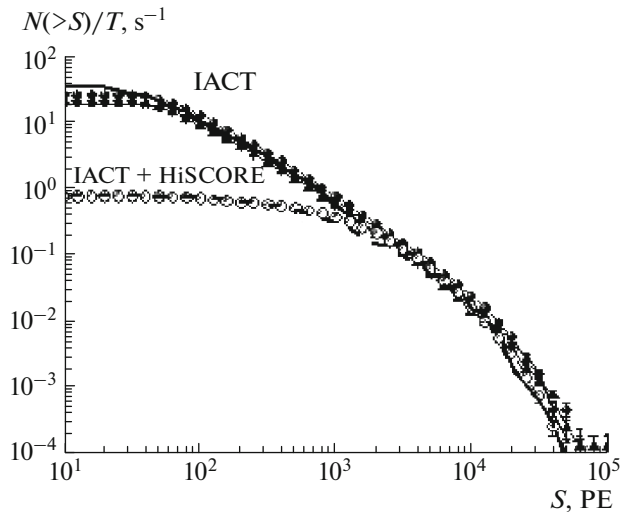


**Fig. 1.** Integral spectrum of size of the images ( $S$ , in photoelectrons) recorded by the IACT over three days, and to joint showers also recorded by the TAIGA-HiSCORE array. Symbols represent the experimental values; the lines, the MC calculations for the corresponding conditions.

for Nuclear Research, Dubna [11]). The simulation allowed for the cluster structure of the telescope camera and the conditions for triggering. Several dozen samples of events corresponding to different tasks were processed. Approximately 30000 events (protons and nuclei), along with 30000 events for primary gamma quanta ( $E\gamma > 40$  TeV), occurred in the energy domain of the hybrid detection of cosmic-ray EASes above 100 TeV.

Figures 1 and 2 show the integral size spectra ( $N_{\text{pix}} \geq 4$ ) for the events during the standalone IACT operation and for the events also detected by the TAIGA-HiSCORE array.

The MC calculations of such a spectrum depend on the chosen primary spectrum. We used the data from the latest experiments (direct and EAS) in the energy range of 100–1000 TeV. The spectrum of all particles was approximated using the function  $F(E) = 13000 \cdot (E/10^4)^{-2.66} \text{ m}^{-2} \text{ s}^{-1} \text{ sr}^{-1} \text{ GeV}^{-1}$ ; of protons and helium,  $F(E) = 7600 \cdot (E/10^4)^{-2.68} \text{ m}^{-2} \text{ s}^{-1} \text{ sr}^{-1} \text{ GeV}^{-1}$ . In simulations, we used a sample of 3–1000 TeV events with a spectral index of  $-2.65$ ; for joint events, the sample was the same but with a threshold of 100 TeV. Comparison of the M-C simulation and the experimental data shows that the energy threshold for detecting proton- and nuclei-initiated EASes during the standalone operation of the telescope is approximately 3 TeV, while the energy threshold for joint events is  $\sim 100$  TeV. On average, EAS energies of approximately 1000 TeV correspond to event sizes of  $\sim 2000$  PE. These are rough estimates, since the size of an event depends strongly on the distance to the EAS axis.

The average lateral distribution functions (LDFs) of the Cherenkov light recorded by the telescope at

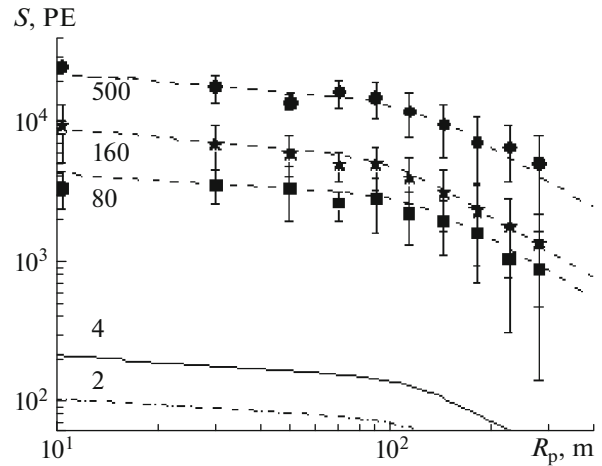


**Fig. 2.** Average image size  $S$  (in photoelectrons) at different distances from the shower axis ( $R_p$ ), obtained from joint events for three energy intervals: 80, 160, and 500 TeV. The two lower curves are extrapolations to proton energies of 4 and 2 TeV, shown for the estimate of the region of threshold detection.

different distances  $S(R_p, E)$  from the shower axis were constructed to obtain a more accurate estimate of the threshold region. The LDFs were determined from joint events with known energy and distance to the shower axis for three energy intervals: 80, 160, and 500 TeV. The LDFs were then extrapolated to the regions of 4 and 2 TeV (the two lower curves in Figs. 3 and 4). In the first approximation, the LDF of protons and helium nuclei with a certain energy is close to that of a gamma ray-initiated shower with half the energy. In other words, we can detect gamma showers with energies of 1–2 TeV in the region up to  $R_p = 100$  m. The threshold is higher for more distant showers.

In [11], a variety of image parameters were compared to MC calculations. The results from our IACT search for showers of gamma rays from the Crab Nebula and blazar Mkr421 in the low-energy region will be published later, when these sources have been observed for at least 50 h.

#### SEARCH FOR GAMMA-LIKE SHOWERS FROM THE CRAB NEBULA IN THE REGION ABOVE 40 TeV

From October to March, the CN can be observed in the array's aperture for up to 3.5 h per night. In the winter of 2017–2018, only 14 days of joint observations of the CN with the telescope and the TAIGA-HiSCORE array were used for analyzing events; the effective time was  $\sim 25$  h. Seventeen thousand events were selected (based on MC simulations, the expected number was 15 000); for 255 of these, the measured angle between the direction of the shower and the one to the source was  $\Theta < 1^\circ$ .

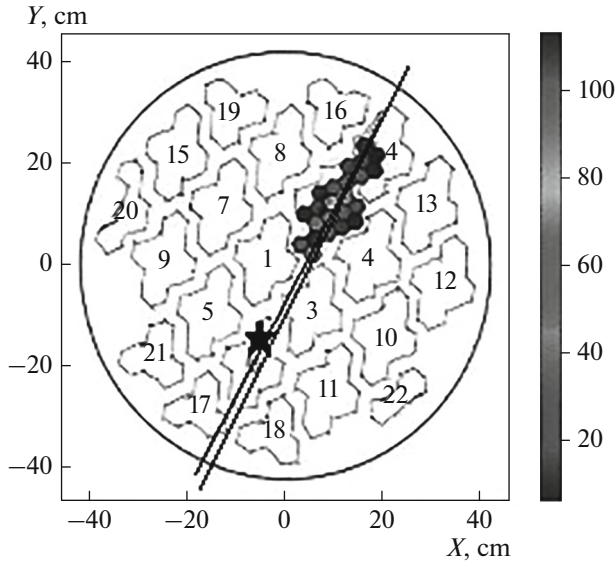


**Fig. 3.** Image of a gamma-like shower in the IACT camera (which has a structure of 22 clusters). The asterisk and line are projections of the shower axis and the point of intersection with the ground on the plane of the telescope camera upon the introduction of scaling factor  $R_p$  (cm)/ $R_c$  (cm); the second line is the major axis of the image, determined using the Hillas algorithm.

The reconstruction of joint events requires the use of parameters determined from the HiSCORE:  $E$ ,  $\theta$ ,  $\varphi$ ,  $R_p$ ; angle  $\Theta$  between the direction of the shower and the one to the source. We also use a number of parameters of the IACT image:  $S$ ,  $R_c$ ,  $W$ ,  $L$ ,  $Con$ , and  $\alpha$  (see Event Reconstruction). For gamma-like events,  $\alpha$  does not exceed  $10^\circ$ – $20^\circ$  and  $W < 0.15^\circ$ , as indicated by MC calculations.

Figure 3 shows an example of a joint gamma-like event recorded by the telescope and the TAIGA-HiSCORE array:  $S = 709$  PE,  $N_{pix} = 23$ ,  $W = 0.13^\circ$ ,  $L = 8.9^\circ$ , and  $\alpha = 8.9^\circ$ . The asterisk in Fig. 3 denotes the projection of the shower axis's position on the plane of the telescope camera upon introducing scaling factor  $R_p$  (cm)/ $R_c$  (cm) = 1500, obtained from the MC calculations for gamma rays. The second line is the major axis of the Hillas ellipse. For events coming from the source to which the telescope is directed, the line connecting the projection of the EAS axis and the center of gravity of the image should cross the center of the camera. The same event was detected by six stations of the TAIGA-HiSCORE array, and the following parameters were determined:  $E = 110$  TeV,  $\theta = 32.9^\circ$ ,  $\varphi = 33.6^\circ$ ,  $R_p = 231$  m. The angle between the direction of the shower, reconstructed using data from the wide-angle array, and the direction to the source was  $\Theta = 0.33^\circ$ . For a rough estimate of the possibility of suppressing the background, Fig. 4 shows the width distributions for joint events with  $S = 1000$ – $3000$  PE, in which showers were selected by the first 30 stations

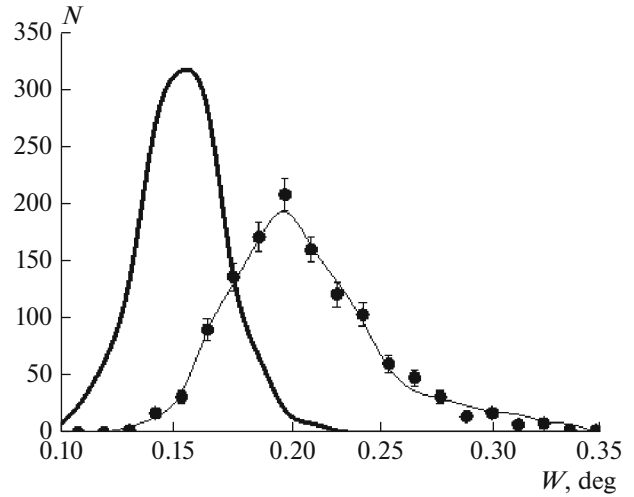


**Fig. 4.** Width distributions of joint events with  $S = 1000$ – $3000$  photoelectrons and MC calculations for a similar sample of events. The solid line shows the calculated width for gamma rays in this sample of sizes.

of the HiSCORE array. This corresponded to short distances to the shower axis and high energies ( $E > 100$  TeV). The line represents the MC simulations for a similar sample of events that describes the experiment quite well. Figure 4 also shows the width calculated for gamma rays in such a sample of sizes. In the first approximation, this ratio of width distributions corresponds to the possibility of suppressing the background by 30 times in only one parameter of width.

From 255 showers with  $\Theta < 1^\circ$ , we selected several gamma-like events that, according to image parameters, could be identified as gamma rays:  $W < 0.16^\circ$ ,  $\alpha < 18^\circ$ , and  $R_c < 3.2^\circ$ . One such event is shown in the figure. The energy of the events was 50–60 TeV, the distance from the axis to the telescope was between 50 and 290 m, and  $\Theta = 0.33^\circ$ – $0.7^\circ$ . The expected number of events from the CN in the energy region above 50 TeV over an area of  $0.25$  km<sup>2</sup>, assuming the gamma-ray spectrum measured in the HEGRA experiment, was 5–10 events in 25 h, which is consistent with our results.

## CONCLUSIONS

Analysis of the operation of the first IACT as part of the TAIGA array in the tracking mode for the CN and blazar Mkr421 showed that events were detected in the direction of a source of high-energy gamma rays with energies above 40 TeV for the first time, using a hybrid approach that combined data from the TAIGA-HiSCORE wide-angle array (with nanosecond measurements of time) and one IACT with image analysis. Approximately 17000 hybrid showers were recorded, and ways of analyzing them were developed.

The parameters obtained experimentally from both arrays were brought to agree with ones obtained in the Monte Carlo simulations.

The threshold energies of gamma rays were estimated for the standalone operation of the telescope (~1–2 TeV) and for the joint events recorded by TAIGA-HiSCORE as well (~40–50 TeV).

Due to a number of technical problems in using the telescope, the time of monitoring the test sources (CN and Mkr421) was ~30 h (instead of the expected 100–120 h). The search results for gamma rays from the two sources in the energy range of 2–10 TeV will be presented later, after at least 50 h of observation. In the range of energies above 50 TeV, approximately 3–7 gamma-like candidates were found using the hybrid approach. Their statistical significance will be determined later.

The area of the TAIGA-HiSCORE observatory will be expanded to 1 km<sup>2</sup> in the 2018–2019 season, and two new telescopes will be added.

#### ACKNOWLEDGMENTS

This work was performed on equipment at the Tunka Astrophysical Center as part of an agreement with the RF Ministry of Science and Higher Education, unique identifier RFMEFI59317X0005.

#### FUNDING

This work was supported by the RF Ministry of Science and Higher Education as part of State Tasks 3.9678.2017/BCh, 3.904.2017/PCh, 3.6787.2017/ITR, and 1.6790.2017/ITR; and by the Russian Foundation for Basic Research, project no. 16-29-13035.

#### REFERENCES

1. Budnev, N.M., Astapov, I.I., Bezyazeev, P.A., et al., *Bull. Russ. Acad. Sci.: Phys.*, 2019, vol. 83, no. 8.
2. Kuzmichev, L.A., Astapov, I.I., Bezyazeev, P.A., Boreyko, V., Borodin, A.N., Budnev, N.M., Wischnewski, R., Garmash, A.Y., Gafarov, A.R., Gorbunov, N.V., Grebenyuk, V.M., Gress, O.A., Gress, T.I., Grinyuk, A.A., Grishin, O.G., et al., *Phys. At. Nucl.*, 2018, vol. 81, no. 4, p. 497.
3. Tluczykont, M., Hampf, D., Horns, D., et al., *Astropart. Phys.*, 2014, vol. 56, p. 42.
4. Bereznev, S.F., Budnev, N.M., Büker, M., Brückner, M., Wischnewski, R., Gafarov, A.V., Gress, O.A., Gress, T., Dyachok, A.N., Epimakhov, S.N., Zagorodnikov, A.V., Zurbanov, V.L., Kalmykov, N.N., Karpov, N.I., Konstantinov, E.N., et al., *Bull. Russ. Acad. Sci.: Phys.*, 2015, vol. 79, no. 3, p. 348.
5. Budnev, N., Astapov, I., Bogdanov, A., et al., *J. Instrum.*, 2014, vol. 9, p. 09021.
6. Kuzmichev, L., Astapov, I., Bezyazeev, P., et al., *EPJ Web Conf.*, 2017, vol. 145, p. 01001.
7. Gres, O., Astapov, I., Bezyazeev, P., et al., *Nucl. Instrum. Methods Phys. Res., Sect. A*, 2017, vol. 845, p. 367.
8. Lubsandorzhev, N., Astapov, I., Bezyazeev, P., et al., *Proc. 35th Int. Cosmic Ray Conf.*, Busan, 2017, p. 757.
9. Zhurov, D., Astapov, I., Bezyazeev, P., et al., *Proc. 35th Int. Cosmic Ray Conf.*, Busan, 2017, p. 785.
10. Hillas, A.M., *Proc. 19th Int. Cosmic Ray Conf.*, La Jolla, 1985, vol. 3, p. 445.
11. Postnikov, E.B., Astapov, I.I., Bezyazeev, P.A., et al., *Bull. Russ. Acad. Sci.: Phys.*, 2019, vol. 83, no. 8.

*Translated by M. Chubarova*